

Weight-adjusted discontinuous Galerkin methods for heterogeneous media and curvilinear meshes

Jesse Chan¹, Russell Hewett², T. Warburton³

¹Department of Computational and Applied Math, Rice University

²TOTAL E&P Research and Technology USA

³Department of Mathematics, Virginia Tech

SIAM CSE
February 28, 2017

High order DG methods for wave propagation

- Unstructured (tetrahedral) meshes for geometric flexibility.
- Low numerical dissipation and dispersion.
- High order approximations: more accurate per unknown.
- High performance on many-core (explicit time stepping).

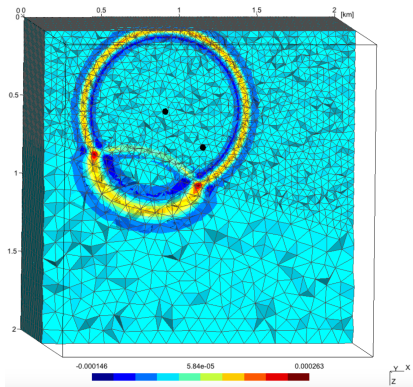
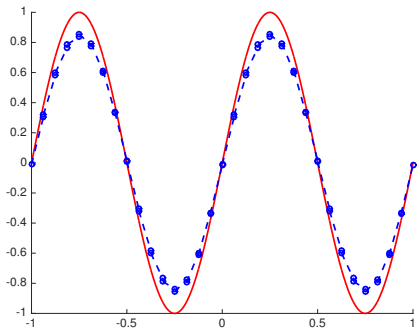


Figure courtesy of Axel Modave.

High order DG methods for wave propagation

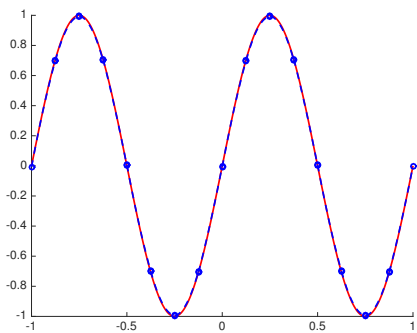
- Unstructured (tetrahedral) meshes for geometric flexibility.
- Low numerical dissipation and dispersion.
- High order approximations: more accurate per unknown.
- High performance on many-core (explicit time stepping).



Fine linear approximation.

High order DG methods for wave propagation

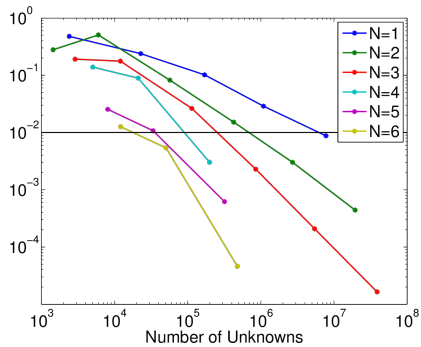
- Unstructured (tetrahedral) meshes for geometric flexibility.
- Low numerical dissipation and dispersion.
- High order approximations: more accurate per unknown.
- High performance on many-core (explicit time stepping).



Coarse quadratic approximation.

High order DG methods for wave propagation

- Unstructured (tetrahedral) meshes for geometric flexibility.
- Low numerical dissipation and dispersion.
- High order approximations: more accurate per unknown.
- High performance on many-core (explicit time stepping).



Max errors vs. dofs.

High order DG methods for wave propagation

- Unstructured (tetrahedral) meshes for geometric flexibility.
- Low numerical dissipation and dispersion.
- High order approximations: more accurate per unknown.
- High performance on many-core (explicit time stepping).



A graphics processing unit (GPU).

Energy stable discontinuous Galerkin formulations

- Model problem: acoustic wave equation

$$\frac{1}{c^2} \frac{\partial p}{\partial t} = \nabla \cdot \mathbf{u}, \quad \frac{\partial \mathbf{u}}{\partial t} = \nabla p$$

- (Local) formulation with penalty fluxes

$$\begin{aligned} \int_{D^k} \frac{1}{c^2} \frac{\partial p}{\partial t} q &= \int_{D^k} \nabla \cdot \mathbf{u} q + \frac{1}{2} \int_{\partial D^k} ([\![\mathbf{u}]\!] \cdot \mathbf{n} + \tau_p [\![p]\!]) q \\ \int_{D^k} \frac{\partial \mathbf{u}}{\partial t} \mathbf{v} &= \int_{D^k} \nabla p \cdot \mathbf{v} + \frac{1}{2} \int_{\partial D^k} ([\![p]\!] + \tau_u [\![\mathbf{u}]\!] \cdot \mathbf{n}) \mathbf{v} \end{aligned}$$

- High order accuracy, semi-discrete energy stability

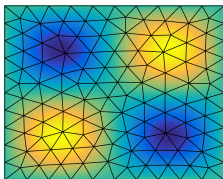
$$\frac{\partial}{\partial t} \left(\sum_k \int_{D^k} \frac{p^2}{c^2} + |\mathbf{u}|^2 \right) = - \int_{\partial D^k} \tau_p [\![p]\!]^2 + \tau_u [\![\mathbf{u} \cdot \mathbf{n}]\!]^2 \leq 0.$$

High order approximation of media and geometry

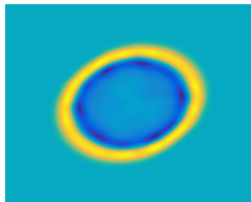
- Efficient implementation on **simplicial** meshes: c^2 piecewise constant, non-curved meshes (J, J^f piecewise constant).

$$\int_{D^k} \frac{1}{c^2} \frac{\partial p}{\partial t} q = \int_{D^k} \nabla \cdot \mathbf{u} q + \frac{1}{2} \int_{\partial D^k} (\llbracket \mathbf{u} \rrbracket \cdot \mathbf{n} + \tau_p \llbracket p \rrbracket) q$$
$$\int_{D^k} \frac{\partial \mathbf{u}}{\partial t} \mathbf{v} = \int_{D^k} \nabla p \cdot \mathbf{v} + \frac{1}{2} \int_{\partial D^k} (\llbracket p \rrbracket + \tau_u \llbracket \mathbf{u} \rrbracket \cdot \mathbf{n}) \mathbf{v}$$

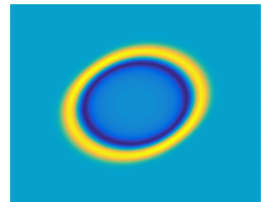
- Spurious reflections for low order approximations of media, geometry.



(a) Mesh and exact c^2



(b) Piecewise const. c^2



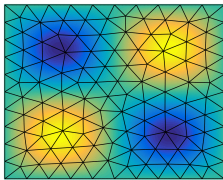
(c) High order c^2

High order approximation of media and geometry

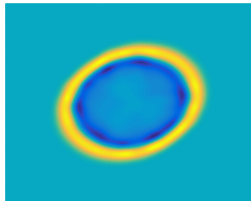
- Efficient implementation on **simplicial** meshes: c^2 piecewise constant, non-curved meshes (J, J^f piecewise constant).

$$\int_{\hat{D}} \frac{1}{c^2} \frac{\partial p}{\partial t} q J = \int_{\hat{D}} \nabla \cdot \mathbf{u} q J + \frac{1}{2} \int_{\partial \hat{D}} ([\![\mathbf{u}]\!] \cdot \mathbf{n} + \tau_p [\![p]\!]) q J^f$$
$$\int_{\hat{D}} \frac{\partial \mathbf{u}}{\partial t} \mathbf{v} J = \int_{\hat{D}} \nabla p \cdot \mathbf{v} J + \frac{1}{2} \int_{\partial \hat{D}} ([\![p]\!] + \tau_u [\![\mathbf{u}]\!] \cdot \mathbf{n}) \mathbf{v} J^f$$

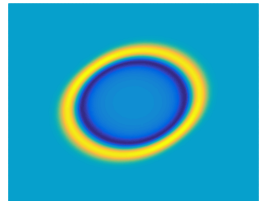
- Spurious reflections for low order approximations of media, geometry.



(a) Mesh and exact c^2



(b) Piecewise const. c^2



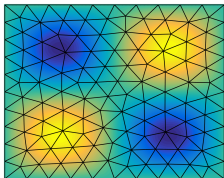
(c) High order c^2

High order approximation of media and geometry

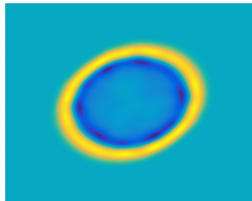
- Efficient implementation on **simplicial** meshes: c^2 piecewise constant, non-curved meshes (J, J^f piecewise constant).

$$\frac{J}{c^2} \int_{\hat{D}} \frac{\partial p}{\partial t} q = J \int_{\hat{D}} \nabla \cdot \mathbf{u} q + J^f \frac{1}{2} \int_{\partial \hat{D}} ([\![\mathbf{u}]\!] \cdot \mathbf{n} + \tau_p [\![p]\!]) q$$
$$J \int_{\hat{D}} \frac{\partial \mathbf{u}}{\partial t} \mathbf{v} = J \int_{\hat{D}} \nabla p \cdot \mathbf{v} + J^f \frac{1}{2} \int_{\partial \hat{D}} ([\![p]\!] + \tau_u [\![\mathbf{u}]\!] \cdot \mathbf{n}) \mathbf{v}$$

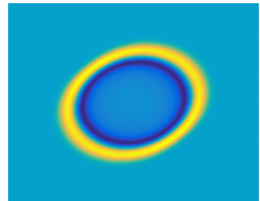
- Spurious reflections for low order approximations of media, geometry.



(a) Mesh and exact c^2



(b) Piecewise const. c^2



(c) High order c^2

Outline

Outline

Weighted mass matrices

- Spatially varying weights appear in DG mass matrices

$$\int_{\hat{D}} \frac{1}{c^2} \frac{\partial p}{\partial t} q J = \text{pressure RHS}, \quad \int_{\hat{D}} \frac{\partial \mathbf{u}}{\partial t} \mathbf{v} J = \text{velocity RHS}$$

- Curvilinear meshes and wave propagation in heterogeneous media

$$(\mathbf{M}_w)_{ij} = \int_{\hat{D}} \phi_i \phi_j w(x),$$

$$\frac{d}{dt} \mathbf{M}_w \mathbf{u} = \text{right hand side.}$$

- Inherits **high order accuracy** and **energy stability** with respect to a weighted L^2 norm, but requires \mathbf{M}_w^{-1} explicitly over each element.
- On-the-fly assembly + inversion or pre-computation and **storage**.

Weighted mass matrices

- Spatially varying weights appear in DG mass matrices

$$\int_{\hat{D}} \frac{1}{c^2} \frac{\partial p}{\partial t} q \mathbf{J} = \text{pressure RHS}, \quad \int_{\hat{D}} \frac{\partial \mathbf{u}}{\partial t} \mathbf{v} \mathbf{J} = \text{velocity RHS}$$

- Curvilinear meshes and wave propagation in heterogeneous media

$$(\mathbf{M}_w)_{ij} = \int_{\hat{D}} \phi_i \phi_j \mathbf{J}(\mathbf{x}),$$

$$\frac{d}{dt} \mathbf{M}_w \mathbf{u} = \text{right hand side.}$$

- Inherits **high order accuracy** and **energy stability** with respect to a weighted L^2 norm, but requires \mathbf{M}_w^{-1} explicitly over each element.
- On-the-fly assembly + inversion or pre-computation and **storage**.

Weighted mass matrices

- Spatially varying weights appear in DG mass matrices

$$\int_{\hat{D}} \frac{1}{c^2} \frac{\partial p}{\partial t} q J = \text{pressure RHS}, \quad \int_{\hat{D}} \frac{\partial \mathbf{u}}{\partial t} \mathbf{v} J = \text{velocity RHS}$$

- Curvilinear meshes and wave propagation in heterogeneous media

$$(\mathbf{M}_w)_{ij} = \int_{\hat{D}} \phi_i \phi_j \frac{J}{c^2(x)},$$

$$\frac{d}{dt} \mathbf{M}_{J/c^2} \mathbf{u} = \text{right hand side.}$$

- Inherits **high order accuracy** and **energy stability** with respect to a weighted L^2 norm, but requires \mathbf{M}_w^{-1} explicitly over each element.
- On-the-fly assembly + inversion or pre-computation and **storage**.

Weighted mass matrices

- Spatially varying weights appear in DG mass matrices

$$\int_{\hat{D}} \frac{1}{c^2} \frac{\partial p}{\partial t} q J = \text{pressure RHS}, \quad \int_{\hat{D}} \frac{\partial \mathbf{u}}{\partial t} \mathbf{v} J = \text{velocity RHS}$$

- Curvilinear meshes and wave propagation in heterogeneous media

$$(\mathbf{M}_w)_{ij} = \int_{\hat{D}} \phi_i \phi_j w(x),$$

$$\frac{d}{dt} \mathbf{M}_w \mathbf{u} = \text{right hand side.}$$

- Inherits **high order accuracy** and **energy stability** with respect to a weighted L^2 norm, but requires \mathbf{M}_w^{-1} explicitly **over each element**.
- On-the-fly assembly + inversion or pre-computation and **storage**.

Weight-adjusted DG: convergence and implementation

- Weight-adjusted DG (WADG): energy stable approximation of weighted mass matrix

$$\mathbf{M}_w \frac{d\mathbf{U}}{dt} \approx \mathbf{M} (\mathbf{M}_{1/w})^{-1} \mathbf{M} \frac{d\mathbf{U}}{dt} = \text{right hand side.}$$

- WADG *a-priori* estimates: standard DG $O(h^{N+1/2})$ convergence of L^2 error based on optimal weighted projection estimate:

$$\|u - P_w u\|_{L^2} \leq Ch^{N+1} \|w\|_{W^{N+1,\infty}} \left\| \frac{\sqrt{J}}{w} \right\|_{L^\infty} \|u\|_{W^{N+1,2}}.$$

- Bypasses inverse of weighted matrix $(\mathbf{M}_w)^{-1}$

$$(\mathbf{M} (\mathbf{M}_{1/w})^{-1} \mathbf{M})^{-1} = \mathbf{M}^{-1} \mathbf{M}_{1/w} \mathbf{M}^{-1}.$$

A non-intrusive and low-storage implementation

- Operator evaluation reuses implementation for $w = 1$

$$\begin{aligned} \mathbf{M} (\mathbf{M}_{1/w})^{-1} \mathbf{M} \frac{d\mathbf{U}}{dt} &= \mathbf{A}_h \mathbf{U} \\ \rightarrow (\mathbf{M}_{1/w})^{-1} \mathbf{M} \frac{d\mathbf{U}}{dt} &= \underbrace{\mathbf{M}^{-1} \mathbf{A}_h \mathbf{U}}_{\text{RHS for } w=1} \end{aligned}$$

- Low storage: matrix-free application of $\mathbf{M}^{-1} \mathbf{M}_{1/w}$.

$$(\mathbf{M})^{-1} \mathbf{M}_{1/w} \text{RHS} = \underbrace{\widehat{\mathbf{M}}^{-1} \mathbf{V}_q^T W \text{diag}(1/w) \mathbf{V}_q}_{P_q} (\text{RHS}).$$

- Non-intrusive: modify RHS locally before update. For non-curved meshes, can combine with *optimal complexity* RHS evaluation.¹

Weight-adjusted DG: not locally conservative

- **Con:** loss of local conservation for $w(x) \notin P^N$!
- **Pro:** superconvergence of conservation error

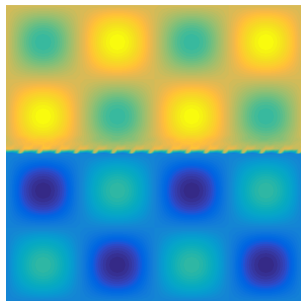
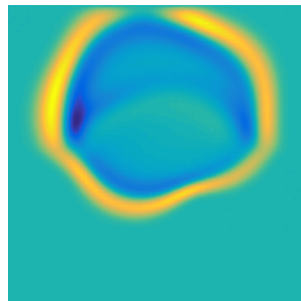
$$\text{Conservation error} \leq Ch^{2N+2} \|w\|_{W^{N+1,\infty}} \|p\|_{W^{N+1,2}}$$

where C depends on mesh quality and max/min values of w .

- **Pro:** can restore local conservation with rank-1 update (Shermann-Morrison).

Outline

Acoustic wave equation: variable coefficients

(a) $c^2(x,y)$ 

(b) Standard DG

Figure: Standard vs. weight-adjusted DG with spatially varying c^2 containing both smooth variations and a discontinuity.

Acoustic wave equation: variable coefficients

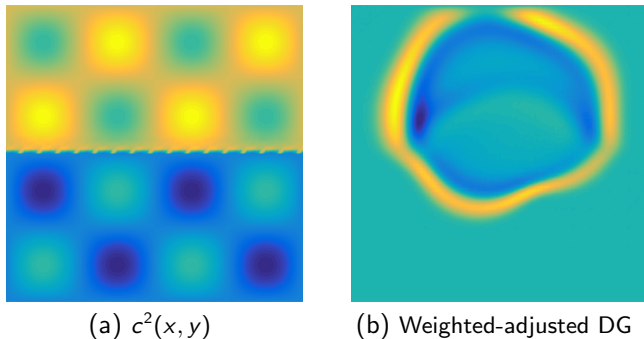


Figure: Standard vs. weight-adjusted DG with spatially varying c^2 containing both smooth variations and a discontinuity.

Acoustics, variable coefficients: L^2 errors

Smooth wavefield $c^2(x, y) = 1 + \frac{1}{2} \sin(\pi x) \sin(\pi y)$

	$h = 1$	$h = 1/2$	$h = 1/4$	$h = 1/8$
DG $N = 1$	2.13e-01	6.25e-02	1.64e-02	4.19e-03
WADG $N = 1$	2.05e-01	5.99e-02	1.62e-02	4.18e-03
DG $N = 2$	3.01e-02	3.60e-03	4.21e-04	5.07e-05
WADG $N = 2$	2.89e-02	3.54e-03	4.18e-04	5.07e-05
DG $N = 3$	6.10e-03	3.33e-04	2.04e-05	1.22e-06
WADG $N = 3$	8.69e-03	3.47e-04	2.03e-05	1.22e-06
DG $N = 4$	6.61e-04	2.12e-05	6.39e-07	1.94e-08
WADG $N = 4$	1.09e-03	2.27e-05	6.30e-07	1.93e-08

Table: Convergence of standard, weight-adjusted DG to a manufactured solution.

Acoustics, variable coefficients: L^2 errors

Smooth wavefield $c^2(x, y) = 1 + \frac{1}{2} \sin(\pi x) \sin(\pi y)$

	$h = 1$	$h = 1/2$	$h = 1/4$	$h = 1/8$
DG $N = 1$	2.48e-01	7.58e-02	1.69e-02	4.46e-03
WADG $N = 1$	2.50e-01	7.72e-02	1.69e-02	4.47e-03
DG $N = 2$	5.95e-02	9.95e-03	1.10e-03	1.22e-04
WADG $N = 2$	6.09e-02	1.02e-02	1.10e-03	1.22e-04
DG $N = 3$	2.29e-02	1.98e-03	9.52e-05	6.56e-06
WADG $N = 3$	1.98e-02	1.98e-03	9.52e-05	6.56e-06
DG $N = 4$	4.90e-03	3.01e-04	1.78e-05	7.27e-07
WADG $N = 4$	4.64e-03	3.02e-04	1.78e-05	7.28e-07

Table: Convergence to a reference solution ($N = 100$ spectral method).

Acoustics, variable coefficients: convergence

	$N = 1$	$N = 2$	$N = 3$	$N = 4$
DG	1.9220	3.0752	4.0440	5.0446
WADG	1.9211	3.0629	4.0752	5.0990

(a) Rates of convergence to manufactured solution

	$N = 1$	$N = 2$	$N = 3$	$N = 4$
DG	1.8256	3.1796	3.8589	4.6171
WADG	1.8425	3.1807	3.8583	4.6128

(b) Rates of convergence to reference solution

Observed L^2 rates between optimal $O(h^{N+1})$ and estimated $O(h^{N+1/2})$.

Outline

Weight-adjusted DG for curvilinear meshes

- Weight-adjusted L^2 projection \tilde{P}_N on curved domains

$$\tilde{P}_N(u) := P_N \left(\frac{1}{J} P_N(uJ) \right).$$

where P_N is the L^2 projection onto the reference element.

- L^2 estimates for weight-adjusted projection:

$$\|u - \tilde{P}_N u\|_{L^2(D^k)} \lesssim \left\| \frac{1}{\sqrt{J}} \right\|_{L^\infty}^2 \|J\|_{W^{N+1,\infty}(D^k)} h^{N+1} \|u\|_{W^{N+1,2}(D^k)}.$$

- High order Sobolev norm of J - implies that convergence can suffer if mapping is not sufficiently regular.

Behavior of weight-adjusted L^2 projection

Comparison with L^2 projection and Low-Storage Curvilinear DG

$$\tilde{\phi}_i = \frac{\phi_i}{\sqrt{J}}, \quad \mathbf{M}_{ij} = \int_{D^k} \tilde{\phi}_j \tilde{\phi}_i J = \int_{\hat{D}} \phi_j \phi_i = \widehat{\mathbf{M}}_{ij}.$$

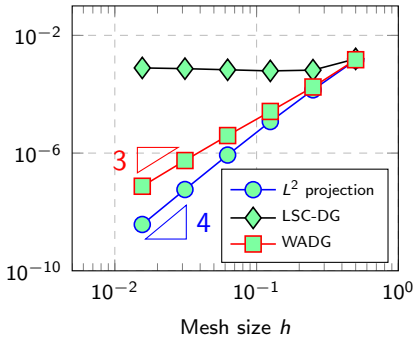
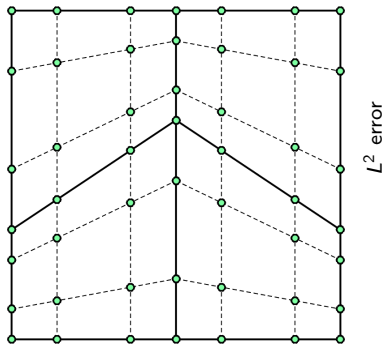


Figure: Arnold-type mesh with $\|J\|_{W^{N+1,\infty}} = O(h^{-1})$ for $N = 3$.

Behavior of weight-adjusted L^2 projection

Comparison with L^2 projection and Low-Storage Curvilinear DG

$$\tilde{\phi}_i = \frac{\phi_i}{\sqrt{J}}, \quad \mathbf{M}_{ij} = \int_{D^k} \tilde{\phi}_j \tilde{\phi}_i J = \int_{\hat{D}} \phi_j \phi_i = \widehat{\mathbf{M}}_{ij}.$$

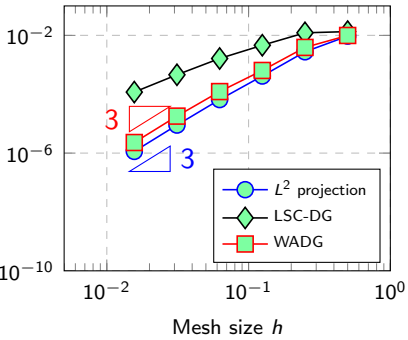
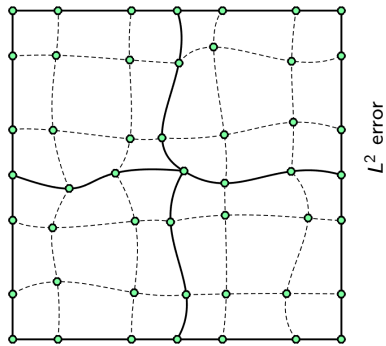
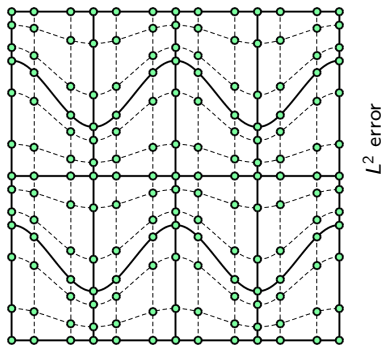


Figure: Curvilinear mesh constructed through random perturbation for $N = 3$.

Behavior of weight-adjusted L^2 projection

High order convergence **slowed** by growth of $\|J\|_{W^{N+1,\infty}} = O(h^N)$.



L^2 error

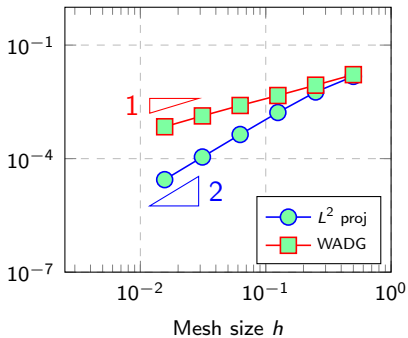
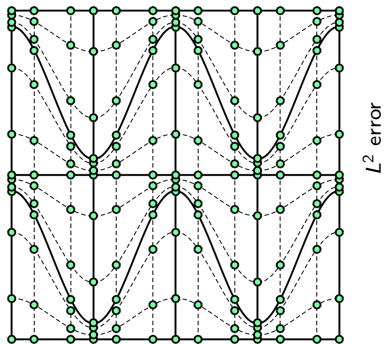


Figure: Moderately warped curved Arnold-type mesh for $N = 3$.

Behavior of weight-adjusted L^2 projection

High order convergence is **stalled** by growth of $\|J\|_{W^{N+1,\infty}} = O(h^{N+1})$.



L^2 error

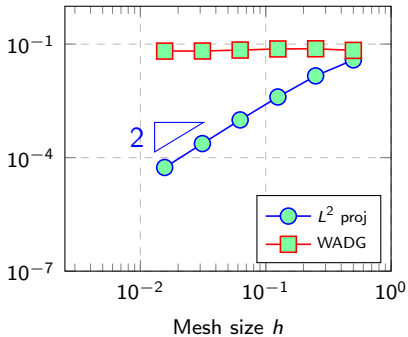
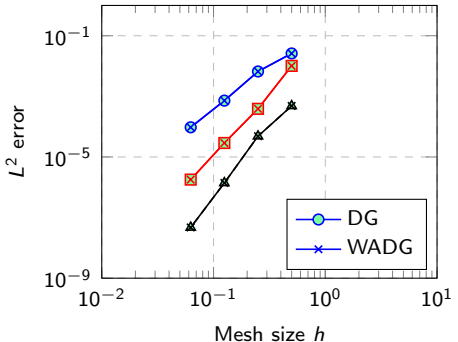
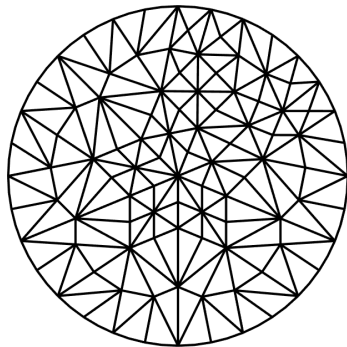


Figure: Heavily warped curved Arnold-type mesh for $N = 3$.

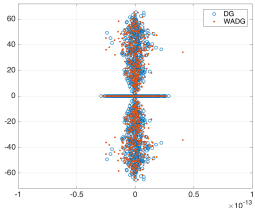
Curvilinear meshes: verification



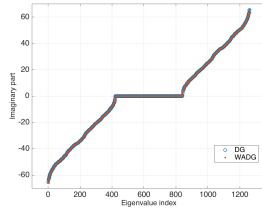
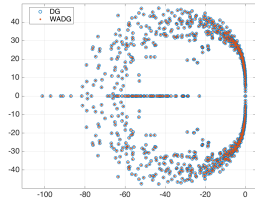
(a) L^2 errors for $N = 2, 3, 4$

Figure: Optimal L^2 convergence rates observed for curvilinear meshes.

Curvilinear meshes: DG eigenvalues (circular domain)



(a) Central fluxes

(b) $\text{Im}(\lambda_i)$ for central fluxes

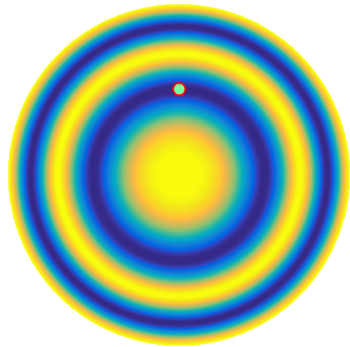
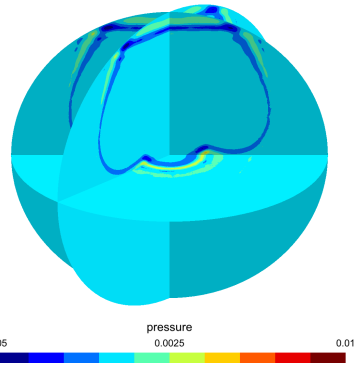
(c) Upwind fluxes

- Energy stability requires quadrature, skew-symmetric formulation

$$\int_{D^k} \frac{\partial p}{\partial t} q = \int_{D^k} -\mathbf{u} \cdot \nabla q + \frac{1}{2} \int_{\partial D^k} (2 \{\{\mathbf{u}\}\} \cdot \mathbf{n} + \tau_p [\![p]\!]) q$$

$$\int_{D^k} \frac{\partial \mathbf{u}}{\partial t} \mathbf{v} = \int_{D^k} \nabla p \cdot \mathbf{v} + \frac{1}{2} \int_{\partial D^k} ([\![p]\!] + \tau_u [\![\mathbf{u}]\!] \cdot \mathbf{n}) \mathbf{v}$$

Curved meshes + heterogeneous media

(a) Wavespeed $c^2(x)$ (b) Pressure isovalues at $t = .6$

Straightforward to combine curved elements and heterogeneous media without compromising efficiency.

Outline

Matrix-valued weights and elastic wave propagation

- Symmetric velocity-stress form of linear elasticity (\mathbf{A}_i constant)

$$\rho \frac{\partial \mathbf{v}}{\partial t} = \sum_{i=1}^d \mathbf{A}_i^T \frac{\partial \boldsymbol{\sigma}}{\partial \mathbf{x}_i}, \quad \mathbf{C}^{-1} \frac{\partial \boldsymbol{\sigma}}{\partial t} = \sum_{i=1}^d \mathbf{A}_i \frac{\partial \mathbf{v}}{\partial \mathbf{x}_i}.$$

- DG formulation based on penalty fluxes, matrix-weighted mass matrix

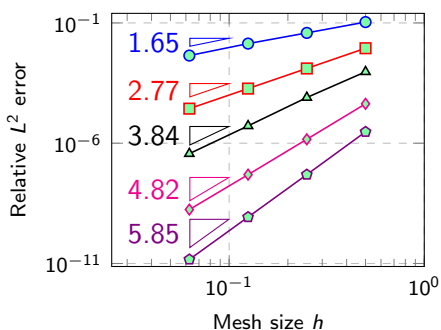
$$(\mathbf{M}_{\mathbf{C}^{-1}})^{-1} = \begin{pmatrix} \mathbf{M}_{C_{11}^{-1}} & \dots & \mathbf{M}_{C_{1d}^{-1}} \\ \vdots & \ddots & \vdots \\ \mathbf{M}_{C_{d1}^{-1}} & \dots & \mathbf{M}_{C_{dd}^{-1}} \end{pmatrix}$$

- Weight-adjusted approximation for \mathbf{C}^{-1} decouples into components

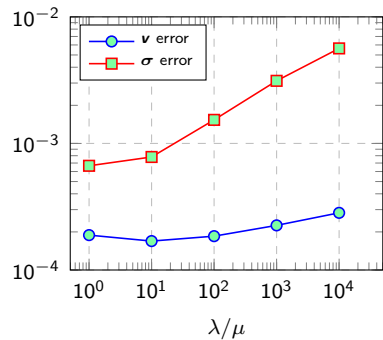
$$\mathbf{M}_{\mathbf{C}^{-1}}^{-1} \approx (\mathbf{I} \otimes \mathbf{M}^{-1}) \mathbf{M}_{\mathbf{C}} (\mathbf{I} \otimes \mathbf{M}^{-1}).$$

Elastic wave propagation: convergence

- Convergence for harmonic oscillation, Rayleigh, Lamb, and Stoneley waves: between $O(h^{N+1})$ and $O(h^{N+1/2})$.
- σ error grows as $\|\mathbf{C}^{-1}\| \rightarrow \infty$ (e.g. incompressible limit $\lambda/\mu \rightarrow \infty$).



(a) Stoneley wave

(b) $\|\mathbf{C}^{-1}\| \rightarrow \infty$, $N = 3, h = 1/8$.

Elastic wave propagation: anisotropy

No change in implementation for anisotropy - fluxes independent of \mathbf{C} .

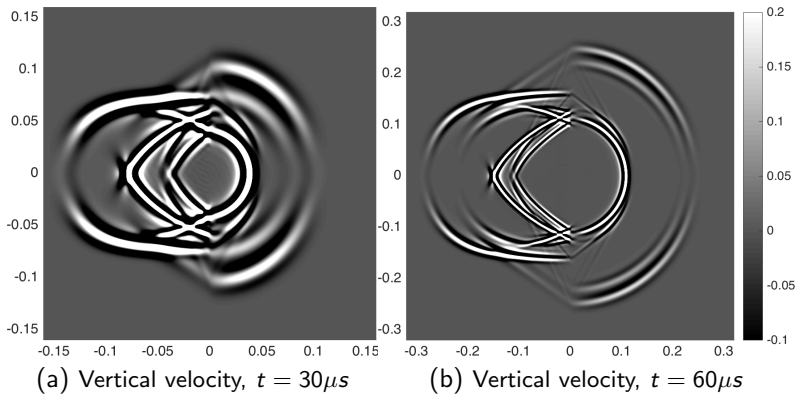


Figure: Heterogeneous media: transverse isotropy ($x < 0$) and isotropy ($x > 0$).

Elastic wave propagation: 3D isotropic media

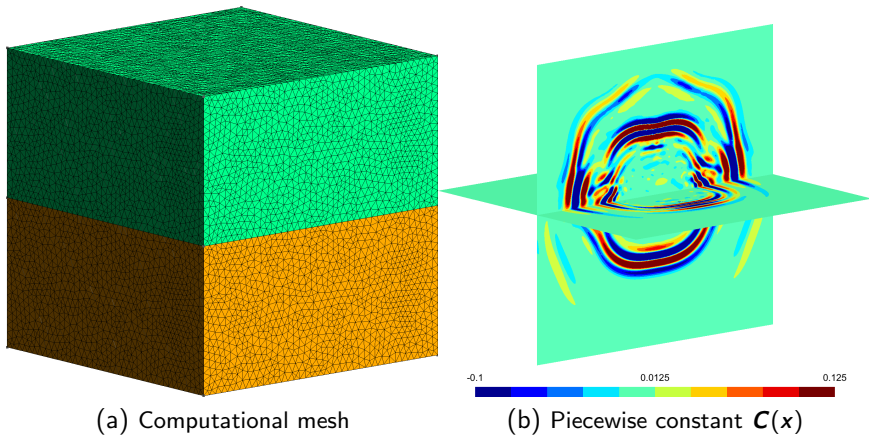


Figure: $\text{tr}(\sigma)$ with $\mu(x) = 1 + H(y) + \frac{1}{2} \cos(3\pi x) \cos(3\pi y) \cos(3\pi z)$, $N = 5$.

Elastic wave propagation: 3D isotropic media

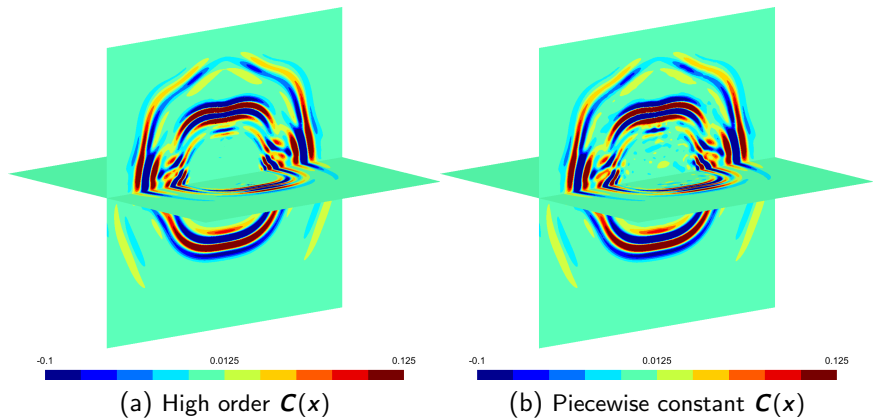


Figure: $\text{tr}(\sigma)$ with $\mu(x) = 1 + H(y) + \frac{1}{2} \cos(3\pi x) \cos(3\pi y) \cos(3\pi z)$, $N = 5$.

Summary and acknowledgements

- Weight-adjusted DG (WADG): **low-storage** methods for heterogeneous media and curvilinear meshes.
- Future directions:
 - Reduce complexity of WADG using Bernstein-Bezier basis.
 - Singular weights (e.g. pyramids)?

Thanks to TOTAL E&P Research and Technology USA
for their support of this work.

Chan, et al. 2016. Weight-adjusted DG methods: wave propagation in heterogeneous media (arXiv).

Chan, et al. 2016. Weight-adjusted DG methods: curvilinear meshes (arXiv).

Chan 2017. Weight-adjusted DG methods: matrix-valued weights and elastic wave prop. in heterogeneous media (arXiv).

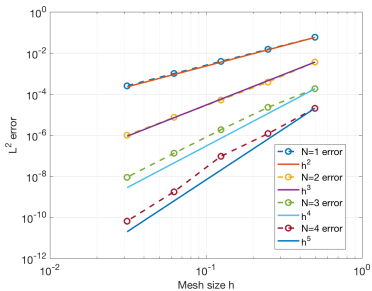
Additional slides

Effect of conservation on shock speeds

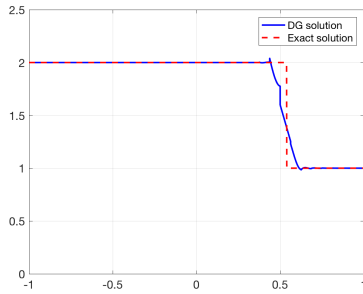
- Weighted Burgers' equation, $w(x)$ curves characteristic lines.

$$w(x) \frac{\partial u}{\partial t} + \frac{1}{2} \frac{\partial u^2}{\partial x} = 0.$$

- WADG yields high order convergence, correct shock speed for both $w(x)$ smooth, discontinuous (within an element).



(a) Smooth solution



(b) Shock solution

Effect of conservation on shock speeds

- Weighted Burgers' equation, $w(x)$ curves characteristic lines.

$$w(x) \frac{\partial u}{\partial t} + \frac{1}{2} \frac{\partial u^2}{\partial x} = 0.$$

- WADG yields high order convergence, correct shock speed for both $w(x)$ smooth, discontinuous (within an element).

Best guess: where and what is locally conserved matters;
non-conservation of *nonlinear flux* results in incorrect shock speeds.

Bernstein-Bezier DG methods

- $O(N^6)$ cost in 3D ($O(N^4)$ with tensor product) vs $O(N^3)$ dofs.
- Sparse Bernstein-Bezier operators (($d + 1$) non-zeros per row).
- Optimal $O(N^3)$ application of derivative and lift.

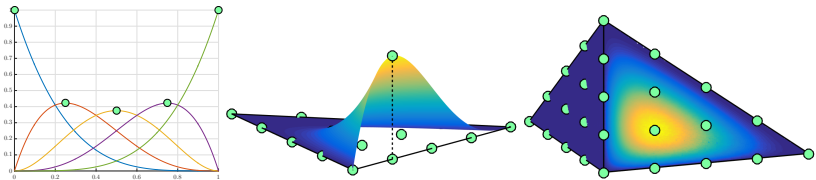


Figure: Bernstein bases in one, two, and three dimensions.

Bernstein-Bezier DG methods

- $O(N^6)$ cost in 3D ($O(N^4)$ with tensor product) vs $O(N^3)$ dofs.
- Sparse Bernstein-Bezier operators (($d + 1$) non-zeros per row).
- Optimal $O(N^3)$ application of derivative and lift.

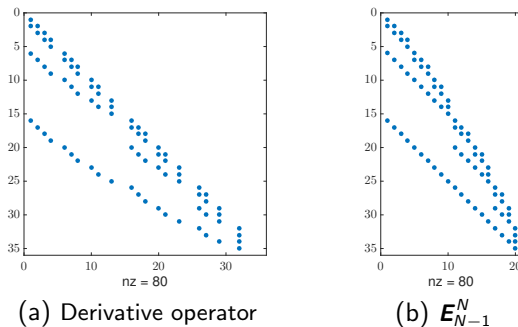


Figure: Sparse Bernstein derivative and degree elevation matrices.

Bernstein-Bezier DG methods

- $O(N^6)$ cost in 3D ($O(N^4)$ with tensor product) vs $O(N^3)$ dofs.
- Sparse Bernstein-Bezier operators (($d + 1$) non-zeros per row).
- Optimal $O(N^3)$ application of derivative and lift.

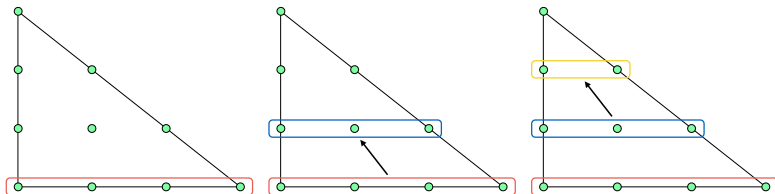


Figure: Optimal-complexity “slice-by-slice” application of Bernstein lift.

Bernstein-Bezier DG methods

- $O(N^6)$ cost in 3D ($O(N^4)$ with tensor product) vs $O(N^3)$ dofs.
- Sparse Bernstein-Bezier operators (($d + 1$) non-zeros per row).
- Optimal $O(N^3)$ application of derivative and lift.

